Antibody repertoire induced by SARS-CoV-2 spike protein immunogens

Supriya Ravichandran, Elizabeth M. Coyle, Laura Klenow, Juanjie Tang, Gabrielle Grubbs, Shufeng Liu, Tony Wang, Hana Golding, and Surender Khurana*

Division of Viral Products, Center for Biologics Evaluation and Research (CBER), FDA, Silver Spring, Maryland, USA, 20871.

One Sentence Summary: SARS-CoV-2 Spike induced immune response

Keywords: SARS-CoV-2, Vaccine, Spike, Neutralization, Epitope, Virus, Antibody, Antigen.

***Corresponding author:**

*Surender Khurana, Ph.D.

Division of Viral Products, Center for Biologics Evaluation and Research (CBER)

Food and Drug Administrationa (FDA)

10903 New Hampshire Avenue

Silver Spring, MD, USA 20993

Phone- 240-402-9632, Fax- (301) 595-1125

E. mail- Surender.Khurana@fda.hhs.gov

ABSTRACT

Multiple vaccine candidates against SARS-CoV-2 based on viral spike protein are under development. However, there is limited information on the quality of antibody response generated following vaccination by these vaccine modalities. To better understand antibody response induced by spike protein-based vaccines, we immunized rabbits with various SARS-CoV-2 spike protein antigens: S-ectodomain (S1+S2) (aa 16-1213), which lacks the cytoplasmic and transmembrane domains (CT-TM), the S1 domain (aa 16-685), the receptor-binding domain (RBD) (aa 319-541), and the S2 domain (aa 686-1213 as control). Antibody response was analyzed by ELISA, Surface Plasmon Resonance (SPR) against different Spike proteins in native conformation, and a pseudovirion neutralization assay to measure the quality and function of the antibodies elicited by the different Spike antigens. All three antigens (S1+S2 ectodomain, S1 domain, and RBD) generated strong neutralizing antibodies against SARS-CoV-2. Vaccination induced antibody repertoire was analyzed by SARS-CoV-2 spike Genome Fragment Phage Display Libraries (SARS-CoV-2 GFPDL), which identified immunodominant epitopes in the S1, S1-RBD and S2 domains. Furthermore, these analyses demonstrated that surprisingly the RBD immunogen elicited a higher antibody titer with 5-fold higher affinity antibodies to native spike antigens compared with other spike antigens. These findings may help guide rational vaccine design and facilitate development and evaluation of effective therapeutics and vaccines against COVID-19 disease.

INTRODUCTION

The ongoing pandemic of SARS-CoV-2 has resulted in more than 2 million human cases and 125,000 deaths as of 15th April 2020. Therefore, development of effective vaccines for prevention and medical countermeasures for treatment of SARS-CoV-2 infection is a high global priority. The spike glycoprotein has been identified as the key target for protective antibodies against both SARS-CoV-1 and SARS-CoV-2(*1-4*). Consequently, multiple versions of the SARS-CoV-2 spike proteins are currently under evaluation as vaccine candidates utilizing different modalities and delivery systems(*5*). However, only limited knowledge exists on antibody repertoire or quality of the immune response generated following vaccination by different spike vaccine antigens. Therefore, it is important to perform comprehensive evaluation of post-vaccination antibody response to elucidate the quality of the immune responses elicited by spike-based vaccine candidates to determine immune markers that may predict clinical benefit which can facilitate evaluation of vaccine candidates.

To better understand vaccination-induced antibody response, we immunized rabbits with several SARS-CoV-2 spike proteins: the S-ectodomain (S1+S2) (aa 16-1213) lacking the cytoplasmic and transmembrane domains (delta CT-TM), the S1 domain (aa 16-685), the receptor-binding domain (RBD) (aa 319-541), and the S2 domain (aa 686-1213), as a control. Post-vaccination sera were analyzed by Genome Fragment Phage Display Libraries covering the entire spike gene (SARS-CoV-2 GFPDL) to determine the polyclonal antibody epitope repertoire generated following vaccination as previously applied for other diseases(*6-10*). In addition, we employed several antibody binding assays (ELISA, Surface Plasmon Resonance (SPR) based real-time kinetics assay) (*10-12*) and an *in vitro* SARS-CoV-2 pseudovirion neutralization assay to measure the quality and function of the antibodies elicited by the different SARS-CoV-2 spike

antigens. This study could inform development and evaluation of SARS-CoV-2 vaccines and therapeutics based on the spike glycoprotein.

RESULTS:

Rabbit immunization with SARS-CoV-2 Spike antigens

Most spike-based vaccines currently under development are designed to contain the receptor-binding domain (RBD; aa 319-541) in some form. Therefore, we evaluated four different commercially available SARS-CoV-2 spike protein and subdomains: the Spike S1+S2 ectodomain (aa 16-1213), the S1 domain (aa 16-685), RBD domain (aa 319-541), and the S2 domain (aa 686-1213) as a control, which is devoid of RBD (Fig. 1A, Suppl. Fig. 1). Theese spike proteins were either produced in HEK 293 mammalian cells (S1 and RBD) or insect cells (S1+S2 ectodomain and S2 domain). The purified S1+S2 ectodomain, the S1 domain, and the RBD proteins retained the functional activity as demonstrated in SPR assay using human ACE2 protein, the SARS-CoV-2 receptor (Fig. 1B). The S1+S2 ectodomain, S1 domain and RBD (black, blue and red binding curves, respectively) demonstrated high-affinity interaction with human ACE2. The control S2 domain protein (green curve), lacking the RBD, did not bind to human ACE2, demonstrating specificity of this receptor-binding assay (Fig.1B).

Female New Zealand white rabbits were immunized twice intra-muscularly at a 14-day interval with 50 μg of the purified proteins mixed with Emulsigen Adjuvant. Sera were collected before (pre-vaccination) and after the first and second vaccination and analyzed for binding antibodies in ELISA and SPR, in a pseudovirion neutralization assay, and by GFPDL analysis.

Antibody Response following immunization with different Spike antigens

Serial dilutions of post-second vaccination rabbit sera were evaluated for binding of serum IgG to various spike proteins and domains in ELISA (S1+S2; black, S1; blue, RBD; red, and S2; green) (Fig. 1C). Representative titration curves to spike ectodomain (S1+S2) and to the RBD in IgG-ELISA are shown in Suppl. Fig. 2. End-point titers of the serum IgG were determined as the reciprocal of the highest dilution providing an optical density (OD) twice that of the negative control (Fig. 1C). All four immunogens elicited strong IgG binding to the spike ectodomain (S1+S2). Binding to the individual domains (S1, S2, and RBD) was specific, in that sera generated by S2 vaccination bound to S2, but not to S1 or RBD, and vice-versa (Fig. 1C).

SPR allows following antibody binding to captured antigens in real-time kinetics, including total antibody binding in resonance units (Max RU) and affinity kinetics (Suppl. Fig. 3). In ELISA, the antigens directly coated in the wells can be partially denatured increasing the likelihood of presenting epitopes that are not seen on the native form of the protein by the polyclonal serum IgG. On the other hand, in our SPR, the purified recombinant spike proteins were captured to a Ni-NTA sensor chip to maintain the native conformation (as determined by ACE2 binding) to allow comparisons of binding to and dissociation from the four proteins. Importantly, the protein density captured on the chip surface is low (200 RU) and was optimized to measure primarily monovalent interactions, so as to measure the average affinity of antibody binding in the polyclonal serum (*8, 13*). Additionally, while ELISA measured only IgG binding, in SPR, all antibody isotypes contributed to antibody binding to the captured spike antigen. In the current study, all rabbit sera contained anti spike antibodies that were at least 86% IgG (data not shown). Serial dilutions of post-vaccination serum were analyzed for binding kinetics with different spike proteins (Suppl. Fig. 3). The spike ectodomain (S1+S2) generated antibodies that predominantly bound to S1+S2

(black bar), followed by the S1 protein (blue bar), and 3-fold lower antibody binding to the RBD and the S2 domain (red and green bars, respectively) (Fig. 1D). The S1 domain antigen induced antibodies that bound with similar titers (Max RU values) to the S1+S2, S1 and RBD proteins (black, blue and red bars, respectively), and did not show reactivity to the S2 domain (green bar). However, the antibody reactivity of rabbit anti-S1 serum to S1+S2 domain was 3-fold lower than the antibodies in the rabbit anti-S1+S2 serum. RBD immunization generated similar high-titer antibody binding to S1+S2, S1 and RBD (black, blue and red bars, respectively), (Fig. 1D). In contrast, the S2 domain induced antibodies that primarily bound to homologous S2 antigen (green bars) and only weakly binding to the S1+S2 ectodomain (black bars), and no binding to either S1 or RBD (Fig. 1D).

Antibody off-rate constants, which describe the fraction of antigen–antibody complexes that decay per second, were determined directly from the serum sample interaction with SARS-CoV-2 spike ectodomain (S1+S2), S1, S2, and RBD using SPR in the dissociation phase only for sensorgrams with Max RU in the range of 20–100 RU (Suppl. Fig. 3) and calculated using the BioRad ProteOn manager software for the heterogeneous sample model as described before(*11*). These off rates provide additional important information on the affinity of the antibodies following vaccination with the different spike proteins that are likely to have an impact on the antibody function *in vivo*, as was observed previously in studies with influenza virus, RSV and Ebola virus (*13-15*). Surprisingly, we observed significant differences in the affinities of antibodies elicited by the four spike antigens (Fig. 1E). Specifically, the RBD induced 5-fold higher affinity antibodies (slower dissociation rates) against S1+S2 (black), S1 (blue) and RBD (red) proteins, compared with the post-vaccination antibodies generated by other three immunogens (Fig. 1E).

131 SARS-CoV-2 neutralization was measured using SARS-CoV-2-FBLuc in a single-cycle
132 PsVN assay in Vero E6 cells. The average percent inhibition by post-first and post-second rabbit
133 vaccination are shown in Fig. 1F. Pre-vaccination rabbit sera (Control Rb) did not neutralize
134 SARS-CoV-2 in PsVN assay. Sera generated by S1+S2-ectodomain, S1 and RBD (1:40 dilution)
135 (but not anti-S2) showed 50-60% virus neutralization after a single vaccination, and 93-98% virus
136 inhibition by the post-second vaccination sera (Fig. 1F).

137

138 **Epitope repertoires recognized by antibodies generated against SARS-CoV-2 spike antigens**

139 The constructed SARS-CoV-2 GFPDL contains sequences ranging from 50-1500 bp long
140 from the spike gene (GenBank #MN908947) with $>10^{7.2}$ unique phage clones. The SARS-CoV-2-
141 GFPDL displayed linear and conformational epitopes with random distribution of size and
142 sequence of inserts that spanned the entire spike gene. SARS-CoV-2 GFPDL panning with
143 individual post-second vaccination rabbit sera were conducted as described in Methods. The
144 numbers of IgG-bound SARS-CoV-2 GFPDL phage clones with different serum sample ranged
145 between 2.6 x 10^4 to 9.8 x 10^5/mL (Fig. 2A). Graphical distribution of representative clones with
146 a frequency of $\geq$2, obtained after affinity selection, and their alignment to the spike protein of
147 SARS-CoV-2 are shown for the four vaccine groups (Fig. 2 B-E). The spike (S1+S2) ectodomain
148 induced diverse antibody response that included strong binding to epitopes in the C-terminal region
149 of the soluble protein spanning the HR2 region (i.e., multiple phage clones with similar inserts).
150 This region may not be highly exposed on the virions or infected cells but is clearly immunogenic
151 in the soluble recombinant spike ectodomain. In addition, the rabbit anti-S1+S2 antibodies bound
152 diverse epitopes spanning the RBD and to a lesser degree to the N-terminal domain (NTD) and the
153 C-terminal region of S1, and the N-terminus of S2, including the fusion peptide (Fig. 2B and Suppl.

Table 1). The S1 domain elicited very strong response against the C-terminal region of S1 protein and a diverse antibody repertoire recognizing the NTD and RBD/RBM regions (Fig. 2C and Suppl. Table 1). The recombinant RBD induced high-titer antibodies that were highly focused to the RBD/RBM (Fig. 2E, and Suppl. Table 1). In contrast, the recombinant S2 immunogen after two immunizations in rabbits elicited antibodies primarily targeting the C-terminus of the S2 protein (CD-HR2).

All the immunodominant antigenic sites identified by the SARS-CoV-2 GFPDL panning of all 4 immune sera on the spike sequence are shown in Suppl. Fig. 4. Alignment of the sequence with other coronaviruses shows that some of the antigenic sites are >70% conserved among several coronavirus strains isolated from humans and bats, especially those located in the S2 domain (Suppl. Table 1). Structural depiction of these antigenic sites on the SARS-CoV-2 spike (Suppl. Fig. 5; in blue on PDB#6VSB), demonstrated that most of these antigenic sites identified in the current study are surface exposed on the native prefusion spike(*2*).

DISCUSSION

In this study, we performed an in-depth evaluation of antibody response generated by various SARS-CoV-2 spike antigens that are similar to the vaccine antigens being used in clinical development(*5, 16, 17*). Bioinformatics approach previously identified 279 potential B-cell epitopes and 48 potential T cell epitopes in the Spike glycoproteins of SARS-CoV viruses, based on human antibody responses to the SARS-CoV-1 infection and the corresponding epitopes in SARS-CoV-2 spike (Grifoni et al. Table 4) (*18*). We compared the predominant antigenic sites identified by antibodies in our study generated by different spike antigens with the B cell epitopes predicted by Grifoni *et al.*(*18*). Four of the predicted B epitopes overlapped with the sequences we

identified in our GFPDL analysis: aa 287-317 in NTD-RBD overlaps with our antigenic site aa 298-363 which is 77% homologous between SARS-CoV-1 and SARS-CoV-2; aa 524-598 and aa 601-640, in the C-terminus of S1 overlap with our antigenic site containing aa 548-632 (78.8 % conservation between SARS-CoV-1 and SARS-CoV-2); aa 802-819 in the S2 domain/FP overlaps with our antigenic site aa 768-828 (83% conserved between SARS-CoV-1 and SARS-CoV-2) (Fig. S4 and Suppl. Table 1). The other epitopes identified in our study cover less conserved sequences between the two SARS-CoV viruses that are unique to the SARS-CoV-2 spike and were not identified in the *in-silico* approach by Grifoni et al.

Surprisingly, the S2 domain doesn't appear to elicit as many neutralizing antibodies as RBD or S1. Although S2 contains the fusion peptide, it does not appear to be as immunogenic, compared with S1 or RBD, in generating binding antibodies to the intact spike (S1+S2) ectodomain, as observed in both IgG ELISA and SPR. Even though we characterized the purified proteins in various assays, there is a possibility that the structure of the antigens used in the study is different from the corresponding authentic spike protein on the surface of SARS-CoV-2 virion particle.

One unexpected finding in this study was the higher affinity of antibodies elicited by the RBD compared with the other spike antigens (S1+S2 ectodomain, S1 and S2 domains). In earlier studies, with vaccines against H7N9 avian influenza we found important correlation between antibody affinity against the hemagglutinin HA1 globular domain and control of virus loads after challenge of ferrets with H7N9 (*19*). In study of patients recovering from Zika virus (ZIKV) infections, their antibody affinity against ZIKV E-DIII correlated with lower clinical scores(*20*). In a large randomised clinical trial of IVIG hyper-enriched for influenza virus antibodies (hIVIG), in adults hospitalised with confirmed influenza A or B infections, a statistically significant

virological benefit and clinical benefit for patients infected with B strains, directly correlated with stronger antibody affinities of the hIVIG for circulating B strains (*14*). In a recent longitudinal study of Ebola virus disease survivor, affinity maturation to Ebola virus GP was associated with a rapid decline in viral replication and illness severity in this patient (*13*). Thus, vaccines that can elicit high affinity antibodies may have a significant advantage for *in-vivo* clinical outcome of SARS-CoV-2 infection and contribute to amelioration of disease in infected individuals. Therefore, in addition to measurements of antibody-binding titers and virus neutralization, this and the previous studies demonstrate the importance of assessments of antibody affinity maturation during SARS-CoV-2 vaccine trials.

In summary, our study highlights the need to perform comprehensive analysis of immune response generated following vaccination or SARS-CoV-2 infection to identify biomarkers of protective immunity. In-depth understanding of quantitative and qualitative aspects of immune responses generated by different spike protein vaccine antigens could aid the development and evaluation of effective SARS-CoV-2 therapeutics and vaccines.

ACKNOWLEDGEMENTS:

We thank Keith Peden and Marina Zaitseva for their insightful review of the manuscript.

Funding: The antibody characterization work described in this manuscript was supported by FDA intramural grant funds. The funders had no role in study design, data collection and analysis, decision to publish, or preparation of the manuscript.

The content of this publication does not necessarily reflect the views or policies of the Department of Health and Human Services, nor does mention of trade names, commercial products, or organizations imply endorsement by the U.S. Government.

AUTHOR CONTRIBUTIONS:

Designed research: S.K.

Performed research: S.R., J. T., E.C., L.K., G. G., S.L., T.W., and S.K.

Conducted Animal study: L.K., G. G., and S.K

SARS-CoV-2 neutralization assays: S.L., and T.W.

Contributed to Writing: H.G. and S.K.

Declaration of Interests: The authors declare no competing interests.

Materials & Correspondence. Correspondence and material requests should be addressed to the corresponding author (S.K.).

Ethics Statement: All animal experiments were approved by the U.S. FDA Institutional Animal Care and Use Committee (IACUC) under Protocol #2008-10. The animal care and use protocol meets National Institutes of Health guidelines.

FIGURE LEGENDS

Figure 1: SARS-CoV-2 spike binding and SARS-CoV-2 neutralization by serum antibodies generated following rabbit immunization with spike antigens. A) Schematic representation of the SARS-CoV-2 spike protein and subdomains. Spike S1+S2 ectodomain (aa 16-1213) lacks the cytoplasmic and transmembrane domains (CT-TM), S1 domain (aa 16-685), RBD domain (aa 319-541), and S2 domain (aa 686-1213), all containing 6x His tag at C-terminus, were produced in either HEK 293 mammalian cells (S1 and RBD) or insect cells (S1+S2 ectodomain and S2 domain). (B) Binding of purified proteins to human ACE2 proteins in SPR. Sensorgrams represent binding of purified spike proteins on His-captured chips to 5 µg/mL human ACE2 protein. (C) Anti-spike reactivity of post-immunization rabbit sera. Serial dilutions of post-second vaccination rabbit sera were evaluated for binding to various spike proteins and domains (S1+S2; black, S1; blue, RBD; red, and S2; green) in ELISA. Representative titration curves are shown in Fig. S2. End-point titers of the serum samples were determined as the reciprocal of the highest dilution providing an optical density (OD) twice that of the negative control (no serum was used as negative control). (D) SPR binding of antibodies from rabbits immunized twice with SARS-CoV-2 antigens to spike protein and domains from SARS-CoV-2 (S1+S2; black, S1; blue, RBD; red, and S2; green). Total antibody binding is represented in resonance units in this figure for 10-fold serum dilution. All ELISA and SPR experiments were performed twice and the researchers performing the assay were blinded to sample identity**.** The variations for duplicate runs of ELISA and SPR were <8% and <5%, respectively. The data shown are average values of two experimental runs. (E) Antibody off-rate constants, which describe the fraction of antigen–antibody complexes that decay per second, were determined directly from the serum/ sample interaction with SARS-CoV-2 spike ectodomain (S1+S2), S1, S2, and RBD using SPR in the dissociation phase only for the

sensorgrams with Max RU in the range of 20–100 RU. (F) Virus neutralization titers were measured against SARS-CoV-2-FBLuc in a single-round pseudovirus neutralization assay in triplicates (see Methods). The average percentage inhibition after the first and second vaccination (1:40 serum dilution) for each group are shown. Pre-vaccination rabbit sera also did not neutralize in PsVN assay (Control Rb).

Figure 2: Antibody repertoires generated by different SARS-CoV-2 spike antigens. (A) Number of IgG-bound SARS-CoV-2 GFPDL phage clones using the post-second vaccination rabbit polyclonal sera from the vaccine groups in Fig 1. (B-E) Graphical distribution of representative clones with a frequency of $\geq$2, obtained after affinity selection, and their alignment to the Spike protein of SARS-CoV-2 are shown for the four vaccine groups: S1+S2 ectodomain (B), S1 (C), S2 domain (D) and S1-Receptor binding domain (RBD) (E). The thickness of each bar represents the frequency of repetitively isolated phage, with the scale shown enclosed in a red box in the respective alignments in each panel. The GFPDL affinity selection data was performed twice. Similar numbers of phage clones and epitope repertoire were observed in both phage display analyses.

SUPPLEMENTAL INFORMATION

Figure S1: Purified SARS-CoV-2 proteins analyzed by SDS-PAGE under reducing and non-reducing conditions.

Figure S2: Anti-spike reactivity of post-vaccination rabbit sera in ELISA.

Figure S3: Steady-state equilibrium analysis of different dilutions of serum antibodies binding to Spike protein by SPR.

Figure S4. Sequence alignment of spike protein from diverse CoV strains.

Figure S5. Structural representation of antigenic sites identified in SARS-CoV-2 using GFPDL analyses.

Supplementary Table 1. Sequence similarity (%) of SARS-CoV-2 spike antigenic sites with other CoV strains.

METHODS:

Recombinant CoV Proteins

Recombinant SARS-CoV-2 proteins were purchased from Sino Biologicals (S1+S2 ectodomain; 40589-V08B1, S1; 40591-V08H, RBD; 40592-V08H or S2; 40590-V08B). Recombinant purified proteins used in the study were either produced in HEK 293 mammalian cells (S1 and RBD) or insect cells (S1+S2 ectodomain and S2 domain).

Rabbit immunization Studies

Female New Zealand white rabbits (Charles River labs) were immunized twice intra-muscularly at 14-days interval with 50 µg of purified proteins mixed with Emulsigen Adjuvant. Sera were collected before (pre-vaccination) and after 1st and 2nd vaccination and analyzed for binding antibodies in ELISA, SPR, neutralization assay and GFPDL analysis.

ELISA

96 well Immulon plates were coated with 100 ng/100 µL of recombinant spike protein and protein domains in PBS overnight at 4ºC. Starting at a 1:100 dilution, serum samples were serially diluted 1:5 and applied to the protein-coated plate in 10 µL for 1 hr at ambient temperature. Serum samples were assayed in duplicate. Naïve serum samples were assayed along with the experimental samples. After three washes with PBS/0.05% Tween 20, bound antibodies were detected with a donkey anti-rabbit IgG Fc-specific HRP-conjugated antibody (Jackson Immuno Research) After

1hr, plates were washed as before and OPD was added for 10min. Absorbance was measured at 492 nm. End titer was determined as 2-fold above the average of the absorbance values of the naïve serum samples. The end titer is reported as the last serum dilution that was above this cutoff.

Antibody binding kinetics of post-vaccination sera to recombinant SARS-CoV-2 proteins by Surface Plasmon Resonance (SPR)

Steady-state equilibrium binding of post-vaccination rabbit polyclonal serum was monitored at 25°C using a ProteOn surface plasmon resonance (BioRad). The purified recombinant Spike proteins were captured to a Ni-NTA sensor chip with 200 resonance units (RU) in the test flow channels. The native functional activity of the Spike proteins was determined by binding to the 5 µg/mL human ACE2 protein.

For serum analysis, the protein density on the chip was optimized such as to measure monovalent interactions independent of the antibody isotype. Serially diluted (10-, 20-, 40-, 80-, and 160-fold of freshly prepared sera were injected at a flow rate of 50 µl/min (120 sec contact duration) for association, and disassociation was performed over a 600-second interval. Responses from the protein surface were corrected for the response from a mock surface and for responses from a buffer-only injection**.** SPR was performed with serially diluted serum of each animal in this study. Antibody isotype analysis for the SARS-CoV-2 spike protein bound antibodies in the polyclonal serum was performed using SPR. Total antibody binding was calculated with BioRad ProteOn manager software (version 3.1). All SPR experiments were performed twice and the researchers performing the assay were blinded to sample identity**.** In these optimized SPR conditions, the variation for each sample in duplicate SPR runs was <5%. The maximum resonance

342 units (Max RU) data shown in the figures was the RU signal for the 10-fold diluted serum sample.
343 Antibody off-rate constants, which describe the fraction of antigen–antibody complexes that decay
344 per second, are determined directly from the serum/ sample interaction with SARS CoV-2 spike
345 ectodomain (S1+S2), S1, S2, and RBD using SPR in the dissociation phase only for the
346 sensorgrams with Max RU in the range of 20–100 RU and calculated using the BioRad ProteOn
347 manager software for the heterogeneous sample model as described before(*11*). Off-rate constants
348 were determined from two independent SPR runs.
349
350 **SARS-CoV-2 pseudovirus production and neutralization assay**
351 Human codon-optimized cDNA encoding SARS-CoV-2 S glycoprotein (NC_045512) was
352 synthesized by GenScript and cloned into eukaryotic cell expression vector pcDNA 3.1 between
353 the BamH*I* and Xho*I* sites. Pseudovirions were produced by co-transfection Lenti-X 293T cells
354 with pMLV-gag-pol, pFBluc, and pcDNA 3.1 SARS-CoV-2 S using Lipofectamine 3000. The
355 supernatants were harvested at 48h and 72h post transfection and filtered through 0.45-mm
356 membranes.
357 For neutralization assay, 50 µL of SARS-CoV-2 S pseudovirions were pre-incubated with
358 an equal volume of medium containing serum at varying dilutions at room temperature for 1 h,
359 then virus-antibody mixtures were added to Vero E6 cells in a 96-well plate. After a 3 h incubation,
360 the inoculum was replaced with fresh medium. Cells were lysed 48 h later, and luciferase activity
361 was measured using luciferin-containing substrate.
362
363 **Gene Fragment Phage Display Library (GFPDL) construction**

SARS-CoV-2 spike gene was chemically synthesized and used for cloning and construction of phage display libraries. A gIII display-based phage vector, fSK-9-3, was used where the desired polypeptide can be displayed on the surface of the phage as a gIII-fusion protein. Purified DNA containing spike gene was digested with *DNase I* to obtain gene fragments of 100-1000 bp size range and used for GFPDL construction as described previously (*6-8*). The phage libraries constructed from the SARS-CoV-2 spike gene display viral protein segments ranging in size from 30 to 350 amino acids, as fusion protein on the surface of bacteriophage.

Affinity selection of SARS-CoV-2 GFPDL phages with polyclonal rabbit serum

Prior to panning of GFPDL with polyclonal serum antibodies, serum components that could non-specifically interact with phage proteins were removed by incubation with UV-killed M13K07 phage-coated petri dishes (*8*). Equal volumes of each post-vaccination rabbit serum were used for GFPDL panning. GFPDL affinity selection was carried out in-solution with protein A/G (IgG) specific affinity resin as previously described (*6, 7, 9*) Briefly, the individual rabbit serum was incubated with the GFPDL and the protein A/G resin, the unbound phages were removed by PBST (PBS containing 0.1 % Tween-20) wash followed by washes with PBS. Bound phages were eluted by addition of 0.1 N Gly-HCl pH 2.2 and neutralized by adding 8 µL of 2 M Tris solution per 100 µL eluate. After panning, antibody-bound phage clones were amplified, the inserts were sequenced, and the sequences were aligned to the SARS-CoV-2 spike gene, to define the fine epitope specificity in the post-vaccination rabbit sera. The GFPDL affinity selection data was performed blindly in a blinded fashion. Similar numbers of bound phage clones and epitope repertoire were observed in the two GFPDL panning.

386

387 **Data Availability**

388 The datasets generated during and/or analyzed during the current study are available from the

389 corresponding author on reasonable request.

390

REFERENCES

1. K. Kuba, Y. Imai, S. Rao, H. Gao, F. Guo, B. Guan, Y. Huan, P. Yang, Y. Zhang, W. Deng, L. Bao, B. Zhang, G. Liu, Z. Wang, M. Chappell, Y. Liu, D. Zheng, A. Leibbrandt, T. Wada, A. S. Slutsky, D. Liu, C. Qin, C. Jiang, J. M. Penninger, A crucial role of angiotensin converting enzyme 2 (ACE2) in SARS coronavirus-induced lung injury. *Nature medicine* **11**, 875-879 (2005).
2. D. Wrapp, N. Wang, K. S. Corbett, J. A. Goldsmith, C. L. Hsieh, O. Abiona, B. S. Graham, J. S. McLellan, Cryo-EM structure of the 2019-nCoV spike in the prefusion conformation. *Science* **367**, 1260-1263 (2020).
3. R. Yan, Y. Zhang, Y. Li, L. Xia, Y. Guo, Q. Zhou, Structural basis for the recognition of SARS-CoV-2 by full-length human ACE2. *Science* **367**, 1444-1448 (2020).
4. A. C. Walls, Y. J. Park, M. A. Tortorici, A. Wall, A. T. McGuire, D. Veesler, Structure, Function, and Antigenicity of the SARS-CoV-2 Spike Glycoprotein. *Cell*, (2020).
5. F. Amanat, F. Krammer, SARS-CoV-2 Vaccines: Status Report. *Immunity*, (2020).
6. S. Khurana, A. L. Suguitan, Jr., Y. Rivera, C. P. Simmons, A. Lanzavecchia, F. Sallusto, J. Manischewitz, L. R. King, K. Subbarao, H. Golding, Antigenic fingerprinting of H5N1 avian influenza using convalescent sera and monoclonal antibodies reveals potential vaccine and diagnostic targets. *PLoS Med* **6**, e1000049 (2009).
7. S. Khurana, W. Chearwae, F. Castellino, J. Manischewitz, L. R. King, A. Honorkiewicz, M. T. Rock, K. M. Edwards, G. Del Giudice, R. Rappuoli, H. Golding, Vaccines with MF59 Adjuvant Expand the Antibody Repertoire to Target Protective Sites of Pandemic Avian H5N1 Influenza Virus. *Science Translational Medicine* **2**, 15ra15-15ra15 (2010).
8. S. Khurana, S. Fuentes, E. M. Coyle, S. Ravichandran, R. T. Davey, Jr., J. H. Beigel, Human antibody repertoire after VSV-Ebola vaccination identifies novel targets and virus-neutralizing IgM antibodies. *Nature medicine* **22**, 1439-1447 (2016).
9. S. Fuentes, E. M. Coyle, J. Beeler, H. Golding, S. Khurana, Antigenic Fingerprinting following Primary RSV Infection in Young Children Identifies Novel Antigenic Sites and Reveals Unlinked Evolution of Human Antibody Repertoires to Fusion and Attachment Glycoproteins. *PLoS Pathog* **12**, e1005554 (2016).
10. S. Khurana, E. M. Coyle, J. Manischewitz, L. R. King, J. Gao, R. N. Germain, P. L. Schwartzberg, J. S. Tsang, H. Golding, C. H. I. C. and the, AS03-adjuvanted H5N1 vaccine promotes antibody diversity and affinity maturation, NAI titers, cross-clade H5N1 neutralization, but not H1N1 cross-subtype neutralization. *NPJ Vaccines* **3**, 40 (2018).
11. S. Khurana, N. Verma, J. W. Yewdell, A. K. Hilbert, F. Castellino, M. Lattanzi, G. Del Giudice, R. Rappuoli, H. Golding, MF59 adjuvant enhances diversity and affinity of antibody-mediated immune response to pandemic influenza vaccines. *Sci Transl Med* **3**, 85ra48 (2011).
12. J. L. Halliley, S. Khurana, F. Krammer, T. Fitzgerald, E. M. Coyle, K. Y. Chung, S. F. Baker, H. Yang, L. Martinez-Sobrido, J. J. Treanor, K. Subbarao, H. Golding, D. J. Topham, M. Y. Sangster, High-Affinity H7 Head and Stalk Domain-Specific Antibody Responses to an Inactivated Influenza H7N7 Vaccine After Priming With Live Attenuated Influenza Vaccine. *J Infect Dis* **212**, 1270-1278 (2015).
13. S. Khurana, S. Ravichandran, M. Hahn, E. M. Coyle, S. W. Stonier, S. E. Zak, J. Kindrachuk, R. T. Davey, Jr., J. M. Dye, D. S. Chertow, Longitudinal Human Antibody Repertoire against Complete Viral Proteome from Ebola Virus Survivor Reveals Protective Sites for Vaccine Design. *Cell Host Microbe* **27**, 262-276 e264 (2020).
14. R. T. Davey, Jr., E. Fernandez-Cruz, N. Markowitz, S. Pett, A. G. Babiker, D. Wentworth, S. Khurana, N. Engen, F. Gordin, M. K. Jain, V. Kan, M. N. Polizzotto, P. Riska, K. Ruxrungtham, Z. Temesgen, J. Lundgren, J. H. Beigel, H. C. Lane, J. D. Neaton, I. F.-I. S. Group, Anti-influenza hyperimmune

437 intravenous immunoglobulin for adults with influenza A or B infection (FLU-IVIG): a double-blind,
438 randomised, placebo-controlled trial. *Lancet Respir Med* **7**, 951-963 (2019).
439 15. S. Fuentes, M. Hahn, K. Chilcote, R. F. Chemaly, D. P. Shah, X. Ye, V. Avadhanula, P. A. Piedra, H.
440 Golding, S. Khurana, Antigenic Fingerprinting of Respiratory Syncytial Virus (RSV)-A-Infected
441 Hematopoietic Cell Transplant Recipients Reveals Importance of Mucosal Anti-RSV G Antibodies
442 in Control of RSV Infection in Humans. *J Infect Dis* **221**, 636-646 (2020).
443 16. T. Thanh Le, Z. Andreadakis, A. Kumar, R. Gomez Roman, S. Tollefsen, M. Saville, S. Mayhew, The
444 COVID-19 vaccine development landscape. *Nat Rev Drug Discov*, (2020).
445 17. W. Tai, L. He, X. Zhang, J. Pu, D. Voronin, S. Jiang, Y. Zhou, L. Du, Characterization of the receptor-
446 binding domain (RBD) of 2019 novel coronavirus: implication for development of RBD protein as
447 a viral attachment inhibitor and vaccine. *Cell Mol Immunol*, (2020).
448 18. A. Grifoni, J. Sidney, Y. Zhang, R. H. Scheuermann, B. Peters, A. Sette, A Sequence Homology and
449 Bioinformatic Approach Can Predict Candidate Targets for Immune Responses to SARS-CoV-2. *Cell*
450 *Host Microbe* **27**, 671-680 e672 (2020).
451 19. S. Khurana, E. M. Coyle, S. Verma, L. R. King, J. Manischewitz, C. J. Crevar, D. M. Carter, T. M. Ross,
452 H. Golding, H5 N-terminal beta sheet promotes oligomerization of H7-HA1 that induces better
453 antibody affinity maturation and enhanced protection against H7N7 and H7N9 viruses compared
454 to inactivated influenza vaccine. *Vaccine* **32**, 6421-6432 (2014).
455 20. S. Ravichandran, M. Hahn, P. F. Belaunzaran-Zamudio, J. Ramos-Castaneda, G. Najera-Cancino, S.
456 Caballero-Sosa, K. R. Navarro-Fuentes, G. Ruiz-Palacios, H. Golding, J. H. Beigel, S. Khurana,
457 Differential human antibody repertoires following Zika infection and the implications for
458 serodiagnostics and disease outcome. *Nat Commun* **10**, 1943 (2019).

459

Fig 1

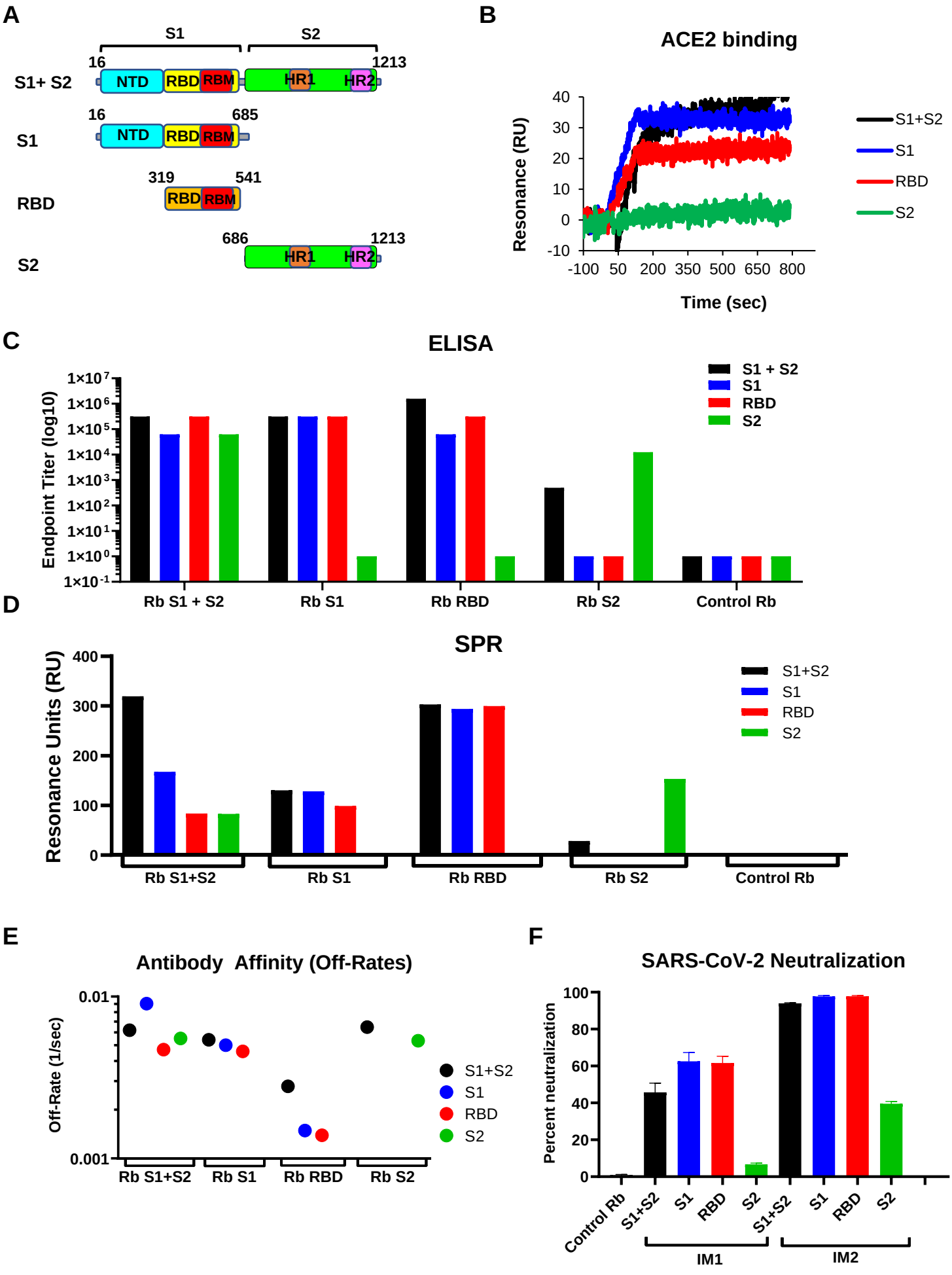

A

	Rb S1+S2	Rb S1	Rb S2	Rb RBD	Control Rb
IgG	5.1E+04	2.2E+05	2.63E+04	9.88E+05	4.20E+01

B

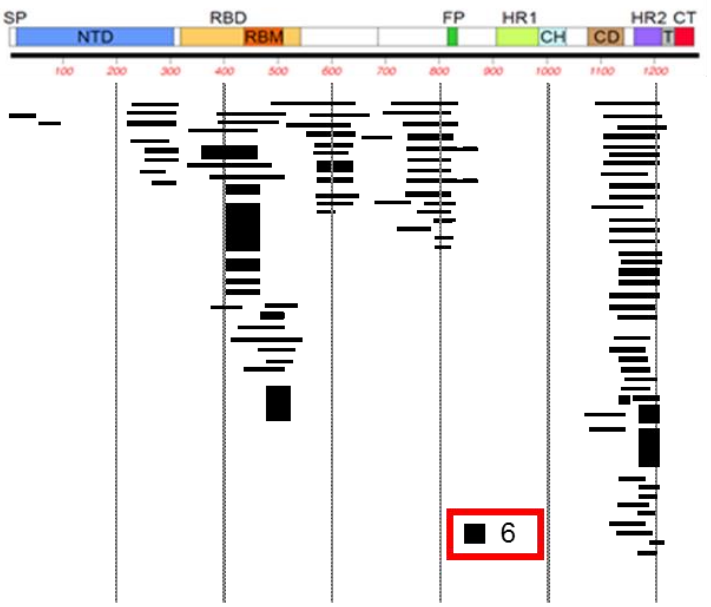

C

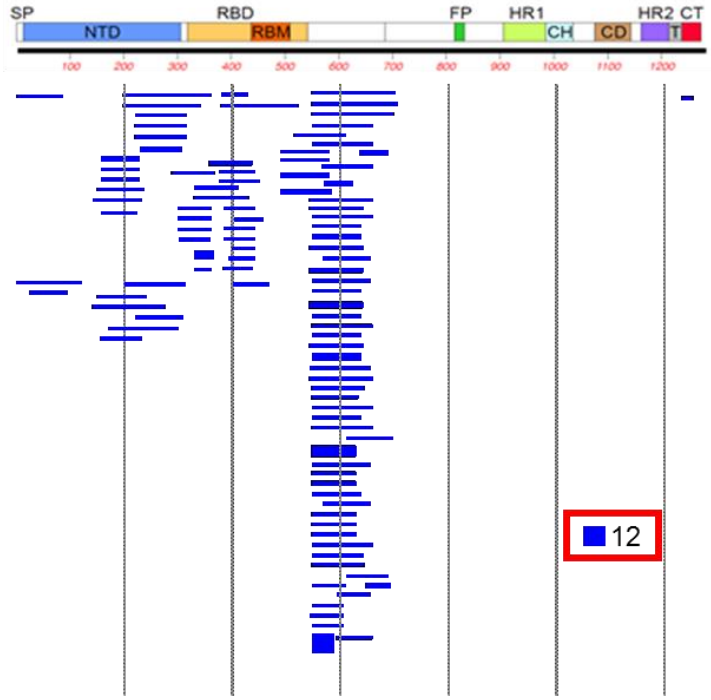

D

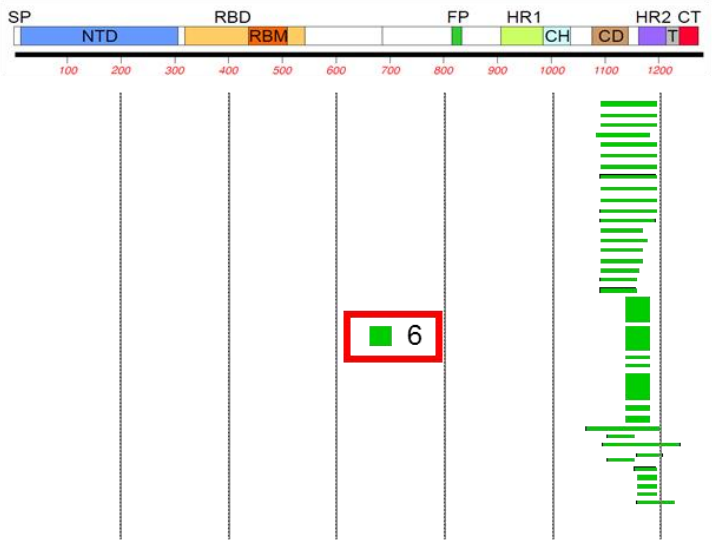

E

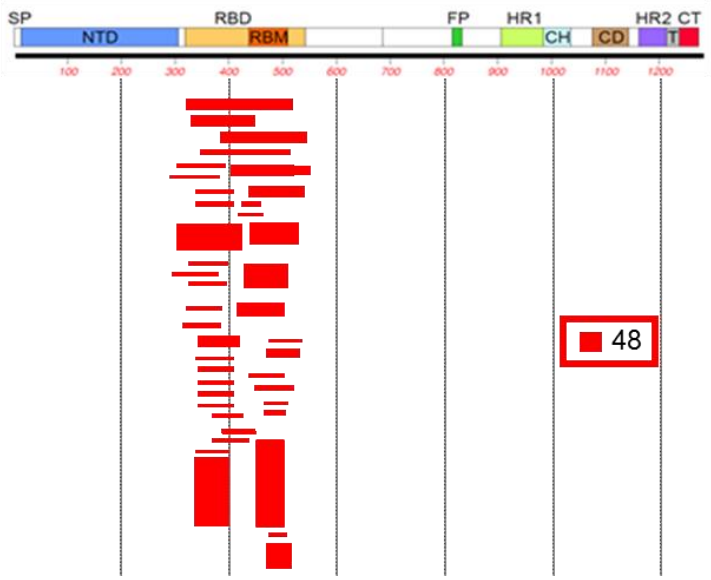

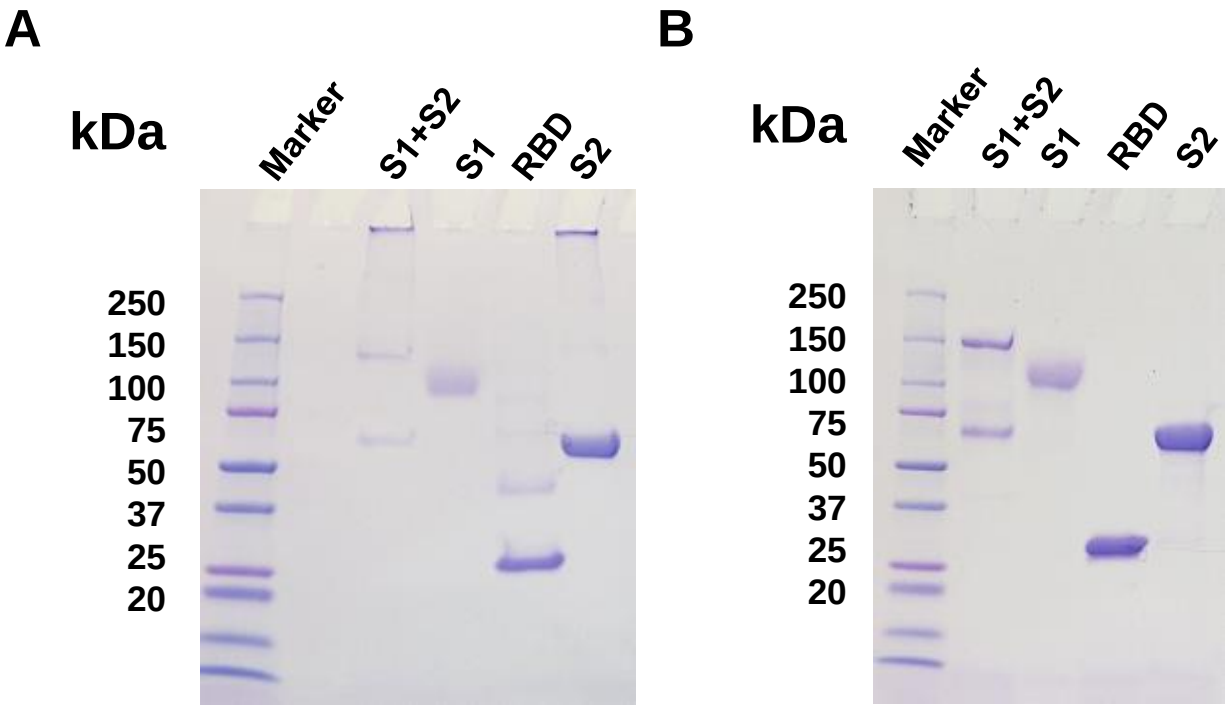

Supplementary Figure 1: Purified SARS-CoV-2 proteins analyzed by SDS-PAGE and under reducing and non-reducing conditions. Related to figure 1. 2 µg of purified proteins was run in SDS-PAGE under non-reducing (A) and reducing (B) conditions. The gels were stained with Coomassie blue.

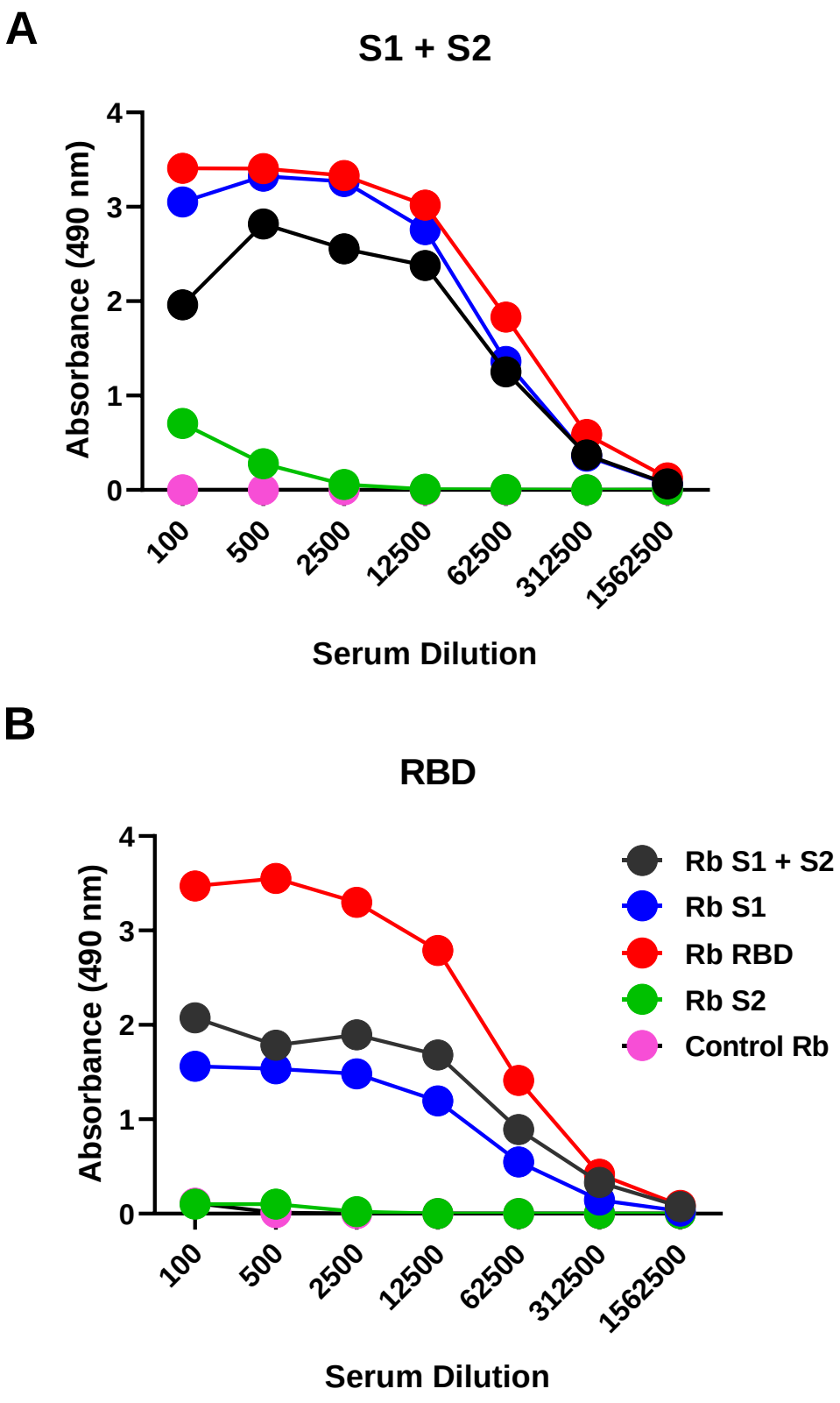

Supplementary Figure 2: Anti-Spike reactivity of post-vaccination rabbit sera in ELISA. Related to figure 1. Post-vaccination rabbit sera following two immunizations with different SARS-CoV-2 spike vaccine antigens (S1+S2; black, S1; blue, RBD; red, S2; green and pre-vaccination control; pink) in ELISA. Average antibody binding to recombinant Spike (S1+S2) ectodomain (A) and S1-RBD (B) is shown in ELISA using HRP-conjugated goat anti-rabbit IgG specific antibody.

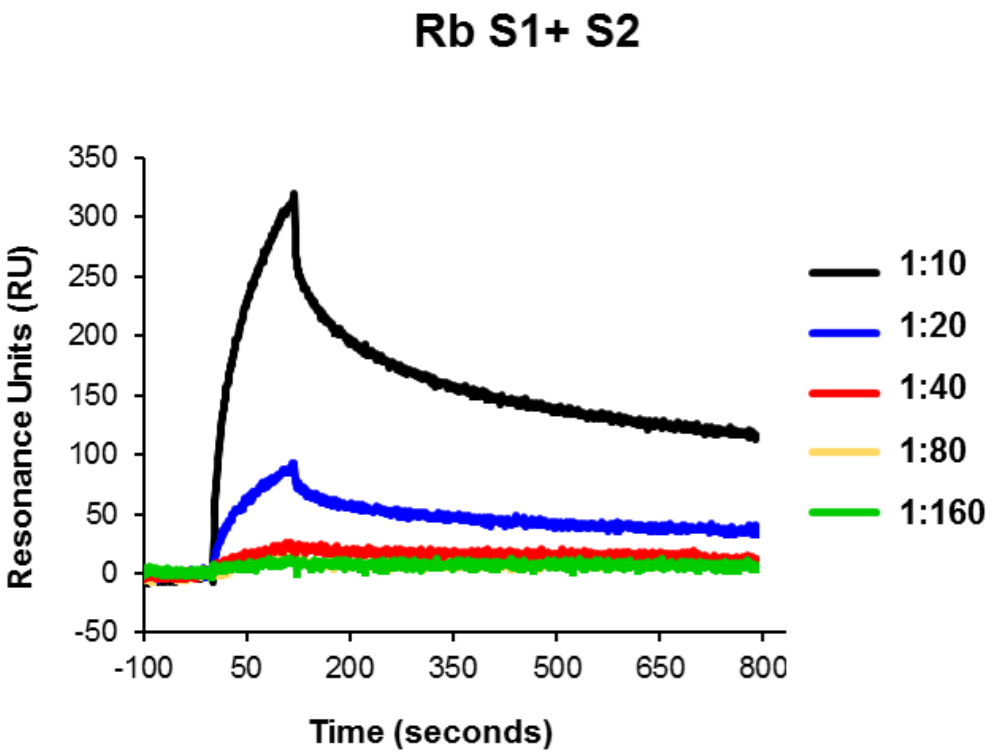

Supplementary Figure 3

Steady-state equilibrium analysis of serum antibodies binding by SPR. Related to figure 1. Serial dilutions of post-2nd vaccination rabbit antiserum against SARS-CoV-2 Spike (S1+S2 ectodomain) were injected simultaneously onto SARS-CoV-1 S1+S2 captured on a Ni-NTA sensor chip and on a surface free of protein (used as a blank). Binding responses from the protein surface were corrected for the response from the mock surface and for responses from a separate, buffer only injection. Unvaccinated Rabbit control sample at 10-fold dilution did not show any binding in SPR.

Supplementary Figure 4. Sequence alignment of Spike protein from diverse CoV strains. Related to figures 1 & 2. An alignment of the spike proteins of SARS-CoV-2 (Genbank#MN908947), SARS-CoV-1 BJ01 strain (Genbank#AAP30030.1), MERS CoV KOR/KNIH/2015(Genbank#AKN11075.1), Bat SARS-like CoV ZC45 (Genbank#AVP78031.1), Bat SARS-like CoV ZXC21 (Genban#AVP78042.1), Bat CoV BM48-31/BGR/2008 (Genbank#ADK66841.1), Human CoV 2c EMC/2012 (Genbank# AFS88936.1), Human CoV NL63 (NCBI#YP_003767.1), and Human CoV HKU1 (NCBI#YP_173238.1) was performed using Clustal W multiple alignment application. Various domains of the spike protein are the S1 subunit (AA 1-685), RBD (AA 319-541), FP (816-834) and S2 (686-1273) subunits. The SARS-CoV-2 antigenic regions/sites discovered in this study using the post-vaccination antibodies with different SARS-CoV-2 vaccine antigens are depicted above the SARS-CoV-2 spike protein sequence in alternating black and grey lines with the corresponding AA residues for visualization.

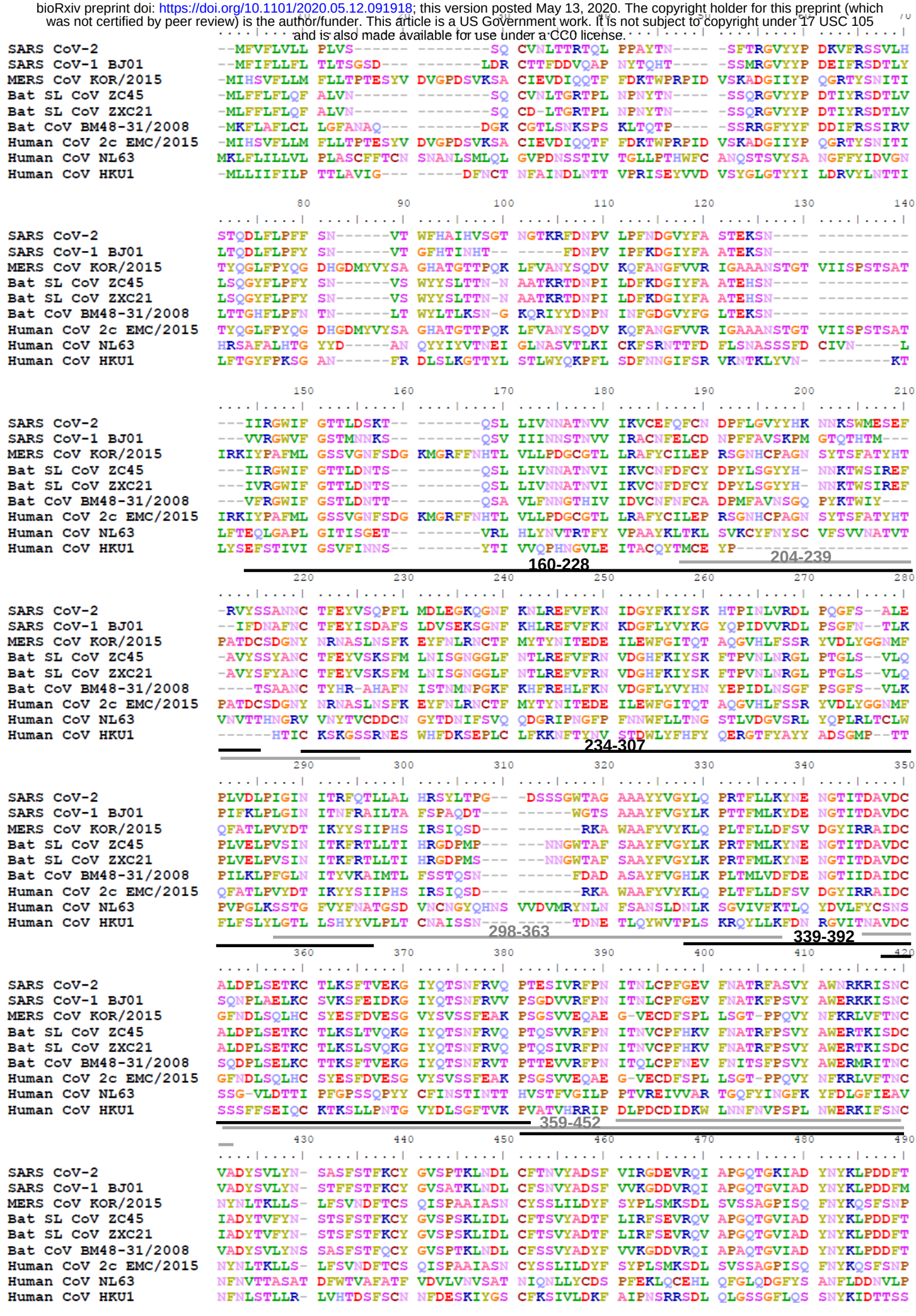

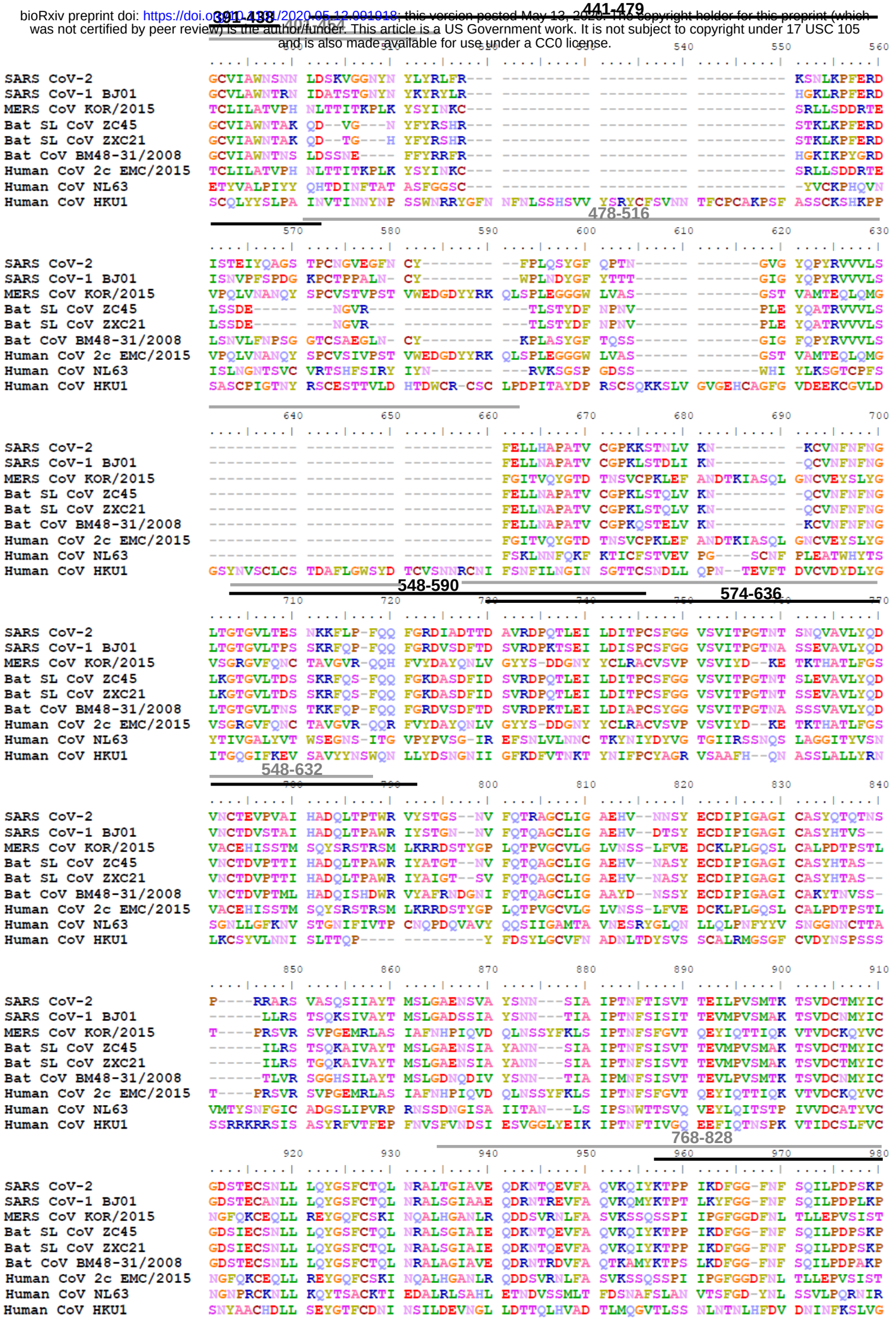

790-834

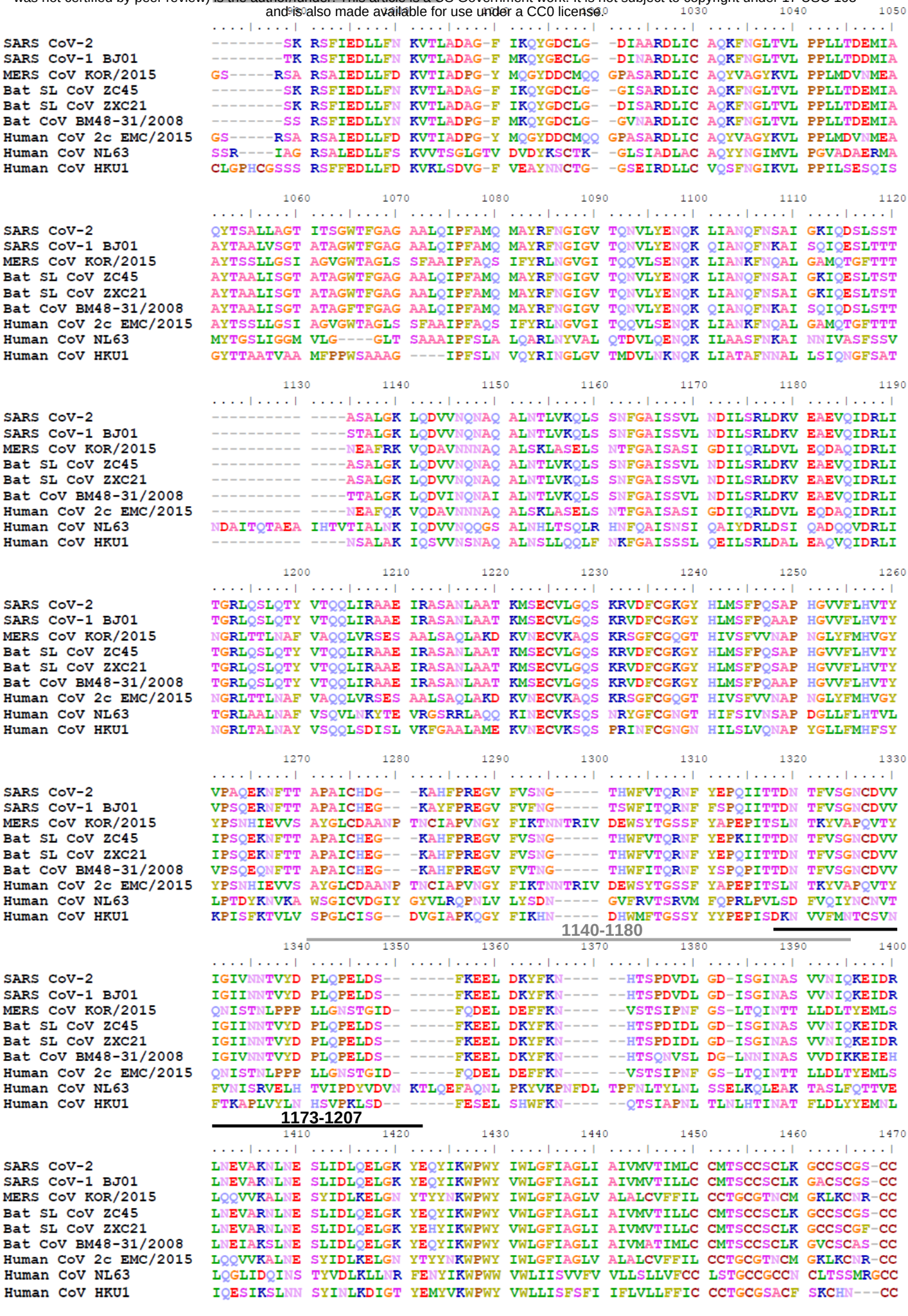

```
                          1455      1460
                          ....|....|  ....|....|
SARS CoV-2                K-FDEDDSEP VLKGVKLHYT
SARS CoV-1 BJ01           K-FDEDDSEP VLKGVKLHYT
MERS CoV KOR/2015         DRYEEYDLEP HKVHVH----
Bat SL CoV ZC45           K-FDEDDSEP VLKGVKLHYT
Bat SL CoV ZXC21          K-FDEDDSEP VLKGVKLHYT
Bat CoV BM48-31/2008      K-FDEDHSEP VLTGVKLHYT
Human CoV 2c EMC/2015     DRYEEYDLEP HKVHVH----
Human CoV NL63            DCGSTKLPYY EFEKVHVQ--
Human CoV HKU1            DEYGGHHDFV IKTSHDD---
```

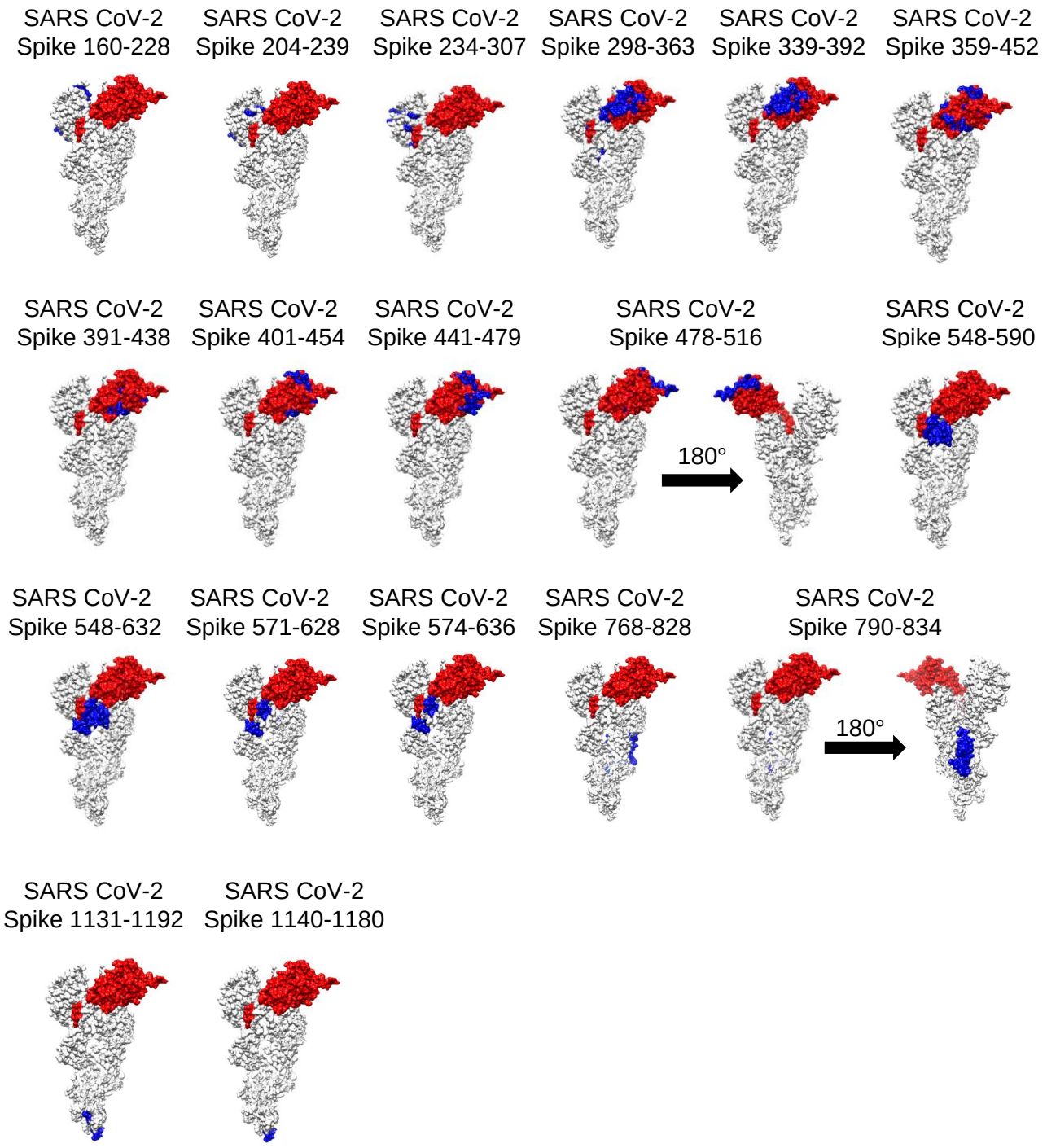

Supplementary Figure 5. Structural representation of antigenic sites identified in SARS-CoV-2 using GFDPL. Related to figure 2. Antigenic sites identified using GFPDL have been depicted in blue on surface structures of a monomer of PDB#6VSB (Wrapp et al., 2020) with a single receptor-binding domain (RBD) in the up conformation, wherever available using UCSF Chimera software. The RBD region is shaded in red (residues 319-541) on every structure. Those structures (SARS CoV-2 Spike 478-516 and 790-834), whose sites were not visible on the side depicted by flipping the structure by 180º.

Table S1: Sequence conservation of Antigenic regions/sites among different CoV strains

AA	Similarity of SARS CoV 2 antigenic sites to other CoV strains (%)								
	SARS CoV-2	SARS CoV-1	MERS	Bat SL CoV ZC45	Bat SL CoV ZXC21	Bat CoV BM48	Human CoV 2c	Human NL63	Human HKU1
160-228	100	53.6	9.7	62.3	60.8	39.1	9.7	12.6	5.7
204-239	100	55.5	10.5	63.8	63.8	44.4	10.5	21	8.1
234-307	100	52.7	32.4	74.3	71.6	48.6	32.4	6.4	27
298-363	100	77.2	30.3	80.3	80.3	78.7	30.3	7.5	30.3
339-392	100	87	24	75.9	75.9	83.6	24	3.6	27
359-452	100	80.8	20.2	74.4	72.3	76.8	20.2	5.2	20.2
391-438	100	83.3	20.8	83.3	83.3	81.2	20.8	8.3	22.9
401-454	100	74	16.6	72.2	68.5	70.3	16.6	5.5	12.9
441-479	100	46.1	10.2	41	35.8	30.7	10.2	10.2	2.7
478-516	100	61.5	14.2	43.5	43.5	56.4	14.2	12.5	8.7
548-590	100	74.4	16.2	74.4	74.4	79	16.2	4.6	22.7
548-632	100	78.8	17.6	80	80	75.2	17.6	4.7	22
574-636	100	80.9	14.2	87.3	87.3	76.1	14.2	3.1	22.2
768-828	100	83.6	41.5	96.7	96.7	80.3	41.5	24.6	24.2
790-834	100	86.6	46.9	100	100	84.4	46.9	32	31.4
1140-1180	100	100	26.1	97.5	97.5	75.6	26.1	14.5	33.3
1173-1207	100	100	45.7	97.1	97.1	82.8	45.7	20	37.1

* Percent sequence conservation of GFPDL identified antigenic sites in the SARS CoV-2 spike protein (Genbank#MN908947), with CoV Spike proteins of SARS CoV-1 BJ01 strain (Genbank#AAP30030.1), MERS CoV KOR/KNIH/2015(Genbank#AKN11075.1), Bat SARS-like CoV ZC45 (Genbank#AVP78031.1), Bat SARS-like CoV ZXC21 (Genban#AVP78042.1), Bat CoV BM48-31/BGR/2008 (Genbank#ADK66841.1), Human CoV 2c EMC/2012 (Genbank# AFS88936.1), Human CoV NL63 (NCBI#YP_003767.1), and Human CoV HKU1 (NCBI#YP_173238.1) was calculated using Sequence Identity Matrix function in BioEdit.